Model order reduction for structural nonlinear dynamic analysis based on Isogeometric analysis

Model order reduction for structural nonlinear dynamic analysis based on Isogeometric analysis

Wei Li, Zhaolin Chen, Yujie Guo*

College of Aerospace Engineering, Nanjing University of Aeronautics and Astronautics, Nanjing 210016, China

Corresponding author's e-mail: yujieguo@nuaa.edu.cn

Abstract. Model order reduction approach generates lower dimensional approximations to the original system while preserving model's essential information and computational accuracy. For nonlinear structural dynamic problems, where the stiffness matrix is configuration dependent, an iterative solution procedure is inevitable and a revisit to all the elements is essential for updating the stiffness matrix. In this paper, the nonlinear dynamics of the planar curved beams and 3D cylindrical shells are studied based on the isogeometric analysis and their model order reductions are investigated based on the proper orthogonal decomposition and discrete empirical interpolation method (POD-DEIM). Numerical results show that IGA-based POD-DEIM method significantly improves the computational efficiency of the nonlinear dynamic analysis of the beam and shell structures.

1. Introduction

Model order reduction approximates the full order system with reduced dimensions while maintaining most of the primary properties of the original system. Proper orthogonal decomposition (POD) is widely used in the reduced order modeling, which generates base vectors and approximates the full order system in a low dimension space. For nonlinear problems where the stiffness matrix is configuration dependent, it is inevitable to revisit all the elements to update the stiffness matrix in each iteration which is not desired for the reduced order modeling[1]. In view of the deficiency of POD, Barrault[2] and Grepl et al.[3] proposed an Empirical Interpolation Method (Empirical Interpolation Method, EIM), it uses a linear combination of base vectors to approximate nonlinear terms where the combination coefficients can be obtained by interpolation. Besides, the base vectors for the ROM are selected based on the greedy algorithm. However, EIM can not be extended to arbitrary nonlinear functions. Chaturanabut et al.[1] proposed a discrete form of EIM, which suits arbitrary ordinary differential equations and is mathematically equivalent to EIM. It uses the selected POD base vectors as input, and DEIM to interpolate the tangent stiffness matrix during the POD model reduction process. Successful example can be found in computational aeroelasticity[4] and structural dynamics[5]. Compared with our previous work[6], this paper expands the reduced order model of nonlinear structural dynamic analysis of Euler-Bernoulli planar curved beams to that of Kirchhoff-Love shells.

Isogeometric analysis (IGA) proposed by Hughes[7] in 2005, uses Non-Uniform Rational B-Splines (NURBS) to describe the geometry and interpolate the physical field, thus unifies CAD and CAE in a integrated sense. IGA has the advantages of accuracy and high-order continuity which is particularly suitable for the analysis and optimization of thin-wall structures. This paper analyzes the nonlinear

dynamic responses of the Euler-Bernoulli planar curved beam[8] and Kirchhoff-Love shell[9] with HHT-α [10] method, and utilizes IGA-based POD-DEIM to construct the reduced-order models of the two systems to verify the feasibility and accuracy of the proposed method.

2. Isogeometric structural analysis

For geometrical nonlinear elastic problems, the governing equations of Euler-Bernoulli planar curved beam and Kirchhoff-Love shell is written as:

$$-\int_A (\boldsymbol{n}:\delta\boldsymbol{\varepsilon}+\boldsymbol{m}:\delta\boldsymbol{\kappa})\mathrm{d}A+\int_A P_0\cdot\delta\boldsymbol{u}\mathrm{d}A+\int_\Gamma \boldsymbol{T}_0\cdot\delta\boldsymbol{u}d\Gamma=\int_A \rho\ddot{\boldsymbol{u}}\cdot\delta\boldsymbol{u}\mathrm{d}A \tag{1}$$

where $\boldsymbol{n}$ is the membrane force, $\boldsymbol{m}$ is the bending moment, $\boldsymbol{\varepsilon}$ is the membrane strain, $\boldsymbol{\kappa}$ is the curvature, $\ddot{\boldsymbol{u}}$ is the second derivative of displacement $\boldsymbol{u}$ w.r.t. time t, A is the analysis domain, ρ is the density, $\mathrm{d}A$ is the differential area in the reference configuration, T_0 and P_0 are the traction along the Neumann boundary Γ and the unit surface load, respectively, which are assumed to be dead loads.

According to the concept of IGA, the displacement $\boldsymbol{u}$ and its variation $\delta\boldsymbol{u}$ can be discretized by the same NURBS basis as the geometry descriptions:

$$\boldsymbol{u}=\sum_{i=1}^{n} R^i\bar{u}^i=\boldsymbol{R}^T\bar{\boldsymbol{u}} \tag{2}$$

$$\delta\boldsymbol{u}=\sum_{i=1}^{n} R^i\delta\bar{u}^i=\boldsymbol{R}^T\delta\bar{\boldsymbol{u}} \tag{3}$$

where R^i is the corresponding NURBS basis, $\bar{u}^i$ and $\delta\bar{u}^i$ represents sets of three unknown values of each control point, $\boldsymbol{R}$ and $\bar{\boldsymbol{u}}$ are the metrices of the corresponding quantities.

Substituting (3) and (2) into (1), the semi-discretized equilibrium equation is obtained as:

$$\boldsymbol{f}_{ext}-\boldsymbol{f}_{\mathrm{int}}=\int_A P_0\cdot\delta\boldsymbol{u}\mathrm{d}A+\int_\Gamma \boldsymbol{T}_0\cdot\delta\boldsymbol{u}d\Gamma-\int_A(\boldsymbol{n}:\delta\boldsymbol{\varepsilon}+\boldsymbol{m}:\delta\boldsymbol{\kappa})\mathrm{d}A=\boldsymbol{M}\ddot{\boldsymbol{u}} \tag{4}$$

$$\boldsymbol{M}=\int_\Omega \rho\boldsymbol{R}^{\boldsymbol{T}}\boldsymbol{R}\mathrm{d}\Omega \tag{5}$$

Where $\boldsymbol{M}$ is the mass matrix, $\boldsymbol{f}_{ext}$ and $\boldsymbol{f}_{\mathrm{int}}$ are the external and internal force vectors, respectively.

The stiffness matrix $\boldsymbol{K}^{\boldsymbol{T}}$ can be obtained by differentiating internal force vector $\boldsymbol{f}_{\mathrm{int}}$ w.r.t. displacement $\boldsymbol{u}$:

$$\boldsymbol{K}^{\boldsymbol{T}}=\int_A\left(\frac{\partial\boldsymbol{n}}{\partial\boldsymbol{u}}:\frac{\partial\boldsymbol{\varepsilon}}{\partial\boldsymbol{u}}+\boldsymbol{n}:\frac{\partial^2\boldsymbol{\varepsilon}}{\partial\boldsymbol{u}\partial\boldsymbol{u}}+\frac{\partial\boldsymbol{m}}{\partial\boldsymbol{u}}:\frac{\partial\boldsymbol{\kappa}}{\partial\boldsymbol{u}}+\boldsymbol{m}\cdot\frac{\partial^2\boldsymbol{\kappa}}{\partial\boldsymbol{u}\partial\boldsymbol{u}}\right)\mathrm{d}A \tag{6}$$

3. POD-DEIM model order reduction

3.1. Concept of model order reduction

Neglecting the effect of damping, the discrete form of the system equilibrium equation can be expressed as:

$$\boldsymbol{M}\ddot{\boldsymbol{u}}+\boldsymbol{K}\boldsymbol{u}=\boldsymbol{f}_{ext} \tag{7}$$

where $\boldsymbol{K}\in\mathbb{R}^{n\times n}$ is the stiffness matrix, $\boldsymbol{M}\in\mathbb{R}^{n\times n}$ is the mass matrix, $\boldsymbol{u}, \boldsymbol{f}_{ext}\in\mathbb{R}^{n\times 1}$.

The solution $\boldsymbol{u}$ can be approximated by a weighted linear combination of a set of orthonormal base vectors $\bar{\boldsymbol{V}}=[\bar{\boldsymbol{v}}_1,\bar{\boldsymbol{v}}_2,\cdots,\bar{\boldsymbol{v}}_k]\in\mathbb{R}^{n\times k}(k\ll n)$:

$$\boldsymbol{u}\approx\sum_{i=1}^{k}\bar{\boldsymbol{v}}_i\bar{u}_i=\bar{\boldsymbol{V}}\bar{\boldsymbol{U}} \tag{8}$$

where $\bar{\boldsymbol{V}}\in\mathbb{R}^{n\times k}$, $\bar{\boldsymbol{U}}\in\mathbb{R}^{k\times 1}$, $\bar{u}_i$ is the generalized displacement. Submit (8) into (7), we can obtain:

$$\boldsymbol{M}\bar{\boldsymbol{V}}\ddot{\bar{\boldsymbol{U}}}+\boldsymbol{K}\bar{\boldsymbol{V}}\bar{\boldsymbol{U}}=\boldsymbol{f}_{ext}+\boldsymbol{r}_{res} \tag{9}$$

where $\boldsymbol{r}_{res}$ is the residual vector generated by the approximation (8). $\boldsymbol{r}_{res}$ span a space that is perpendicular to the subspace spanned by $\bar{\boldsymbol{V}}$, that is $\bar{\boldsymbol{V}}^T\boldsymbol{r}_{res}=0$. Multiplying (9) to the left by $\bar{\boldsymbol{V}}^T$, one can obtain the reduced form of the governing equation:

$$\underbrace{\bar{\boldsymbol{V}}^T\boldsymbol{M}\bar{\boldsymbol{V}}}_{\bar{\boldsymbol{M}}}\ddot{\bar{\boldsymbol{U}}}+\underbrace{\bar{\boldsymbol{V}}^T\boldsymbol{K}\bar{\boldsymbol{V}}}_{\bar{\boldsymbol{K}}}\bar{\boldsymbol{U}}=\underbrace{\bar{\boldsymbol{V}}^T\boldsymbol{f}_{ext}}_{\bar{\boldsymbol{f}}_{ext}}+\underbrace{\bar{\boldsymbol{V}}^T\boldsymbol{r}_{ROM}}_{0} \tag{10}$$

where $\bar{\boldsymbol{M}},\bar{\boldsymbol{K}}\in\mathbb{R}^{k\times k}$, $\boldsymbol{f}_{ext}\in\mathbb{R}^{k\times 1}$.

3.2. Proper orthogonal decomposition

The set of orthonormal base vectors $\bar{\boldsymbol{V}}$ are computed by the Proper Othogonal Decomposition (POD) method. In full order model analysis, the snapshots of the displacement and stiffness matrices are collected and assembled to the matrices $\boldsymbol{U}_{snap}=[\boldsymbol{u}_1,\boldsymbol{u}_2,\cdots,\boldsymbol{u}_{N_s}]$ and $\boldsymbol{K}_{snap}=[\tilde{\boldsymbol{K}}_1,\tilde{\boldsymbol{K}}_2,\cdots,\tilde{\boldsymbol{K}}_{N_s}]$, where $\tilde{\boldsymbol{K}}_i$ is the vectorized form of its original square stiffness matrix $\boldsymbol{K}_i$. Then apply the Singular Value Decomposition (SVD) to the snapshots $\boldsymbol{U}_{snap}$:

$$\mathrm{SVD}(\boldsymbol{U}_{snap})=\boldsymbol{V}\boldsymbol{\Sigma}\boldsymbol{W} \tag{11}$$

where $\boldsymbol{V}\in\mathbb{R}^{n\times N_s}=[\boldsymbol{v}_1,\boldsymbol{v}_2,\cdots,\boldsymbol{v}_{N_s}]$ is the left-hand matrix consisting of a set of orthonormal vectors, $\boldsymbol{W}\in\mathbb{R}^{N_s\times N_s}$ is the right-hand matrix, $\boldsymbol{\Sigma}\in\mathbb{R}^{N_s\times N_s}=\mathrm{diag}(\sigma_1,\sigma_2,\cdots,\sigma_{N_s})$ is the diagonal matrix and $\sigma_1\geq\sigma_2\geq\cdots\geq\sigma_{N_s}>0$. The magnitude of each singular value represents the contribution of the corresponding left basis orthogonal vector to the energy of the entire system. n is the degree of freedom of the system, N_s is the total number of snapshot vectors.

If k base vectors are selected to construct the reduced order model, its approximation error to the snapshots in the sense of least square can be expressed as:

$$\sum_{j=1}^{N_s}\left\|\boldsymbol{U}^j-\sum_{i=1}^{k}(\boldsymbol{v}_i{}^T\boldsymbol{U}^j)\boldsymbol{v}_i\right\|_2^2=\sum_{i=k+1}^{N_s}\sigma_i^2 \tag{12}$$

Then we can choose the number of base vectors according to the following criterial:

$$\sum_{i=k+1}^{N_s}\sigma_i^2\Big/\sum_{i=1}^{N_s}\sigma_i^2\leq\tau \tag{13}$$

where $\tau\in[0,1]$ represents the relative error of the selected base vectors approximating the original system represented by the captured snapshots.

3.3. Discrete Empirical Interpolation Method

To further accelerate the computational speed, discrete empirical interpolation method is used to interpolate the stiffness matrix with nonzero-values at selected locations. Suppose that the stiffness column vector $\tilde{\boldsymbol{K}}_i$ is attracted to a lower-dimensional subspace spanned by $\boldsymbol{h}=[\boldsymbol{\zeta}_1,\boldsymbol{\zeta}_2,\cdots,\boldsymbol{\zeta}_m]\in\mathbb{R}^{n*n\times m}, m\ll n*n$, where $\boldsymbol{h}$ can be obtained by SVD($\boldsymbol{K}_{snap}$) and formula (13). The stiffness column vector can be approximated by a weighted linear combination of the base vectors spanning $\boldsymbol{h}$:

$$\tilde{\boldsymbol{K}}_i\approx\hat{\boldsymbol{K}}_i=\boldsymbol{h}\boldsymbol{c} \tag{14}$$

where $\boldsymbol{c}\in\mathbb{R}^m$ is a set of scalar weight coefficients corresponding to $\boldsymbol{h}$. Since formula (14) is over-constrained, Boolean matrix $\boldsymbol{P}\in\mathbb{R}^{n*n\times m}$ is used where m rows in $\boldsymbol{h}$ are selected:

$$\boldsymbol{P}^T\tilde{\boldsymbol{K}}_i\approx\boldsymbol{P}^T\hbar\boldsymbol{c} \tag{15}$$

Submitting $\boldsymbol{c}$ of (15) into (14) yields the approximated stiffness vector $\hat{\boldsymbol{K}}_i$:

$$\hat{\boldsymbol{K}}_i = \boldsymbol{hc} = \underbrace{\boldsymbol{h}(\boldsymbol{P}^T\boldsymbol{h})^{-1}\boldsymbol{P}^T}_{\boldsymbol{D}}\tilde{\boldsymbol{K}}_i \tag{16}$$

where $\boldsymbol{D}$ is the interpolation matrix, and where Boolean matrix $\boldsymbol{P}$ and the position vector $\boldsymbol{\Phi}$ can be computed with Algorithm 1:

Algorithm 1 DEIM Algorithm

Input: $\boldsymbol{h} = [\zeta_1, \zeta_2, \cdots, \zeta_m] \in \mathbb{R}^{n*n\times m}$

Output: $\boldsymbol{\Phi} = [\phi_1, \phi_2, \cdots, \phi_m]^T \in \mathbb{R}^m$

$[\rho, \phi_1] = \max\{|\zeta_1|\}$

$\boldsymbol{h} = [\xi_i], \boldsymbol{P} = [\boldsymbol{e}_{\phi_i}], \boldsymbol{\Phi} = [\phi_i]$

for $i = 2, \cdots, m$

solve $(\boldsymbol{P}^T\boldsymbol{h})\boldsymbol{c} = \boldsymbol{P}^T\zeta_i$

$\boldsymbol{r}_{residue} = \zeta_i - \boldsymbol{hc}$

$[\rho, \phi_i] = \max\{|\boldsymbol{r}_{residue}|\}$

update: $\boldsymbol{h} = [\boldsymbol{h}, \zeta_i], \boldsymbol{P} = [\boldsymbol{P}, \boldsymbol{e}_{\phi_i}], \boldsymbol{\Phi} = [\boldsymbol{\Phi}^T, \phi_i]^T$

4. Numerical examples

In this section, we consider two examples: the Archimedes spiral curved beam and the 3D cylindrical shell. In the HHT-α method[10], a specific set of parameters ($\alpha = 0$, $\beta = 0.25(1-\alpha)^2$, $\gamma = 0.5-\alpha$, the convergence criteria $tol = 1e-3$) is considered.

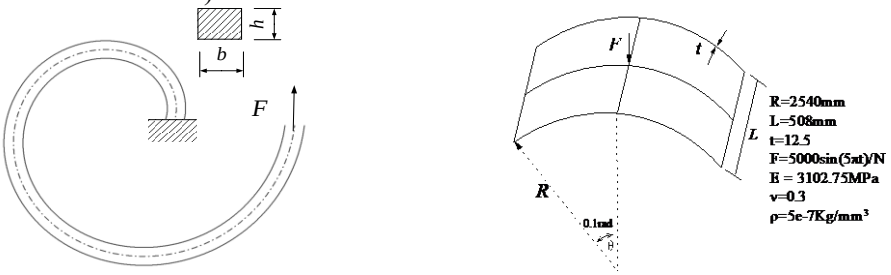

(a) The Archimedes spiral curved beam (b) Four-edge simple supported cylindrical shell

Figure 1. The geometry description

4.1. Archimedes spiral curved beam

This example considers an Archimedes spiral curved beam fixed at one end, the function of geometry description is $r = 5 + 2\theta, \theta \in [0, 2\pi]$ shown in Fig1(a). The beam is subjected to a concentrated force $F = 10\sin(t)\text{N}$ at its free end, the width *b* and height *h* of the cross section equal to 0.5m. The material properties are taken as follows: Yong's modulus $E = 1.2\times10^6\,\text{Pa}$, mass density per unit volume $\rho = 1\text{Kg/m}^3$. The polynomial order of NURBS is *p*=3 and a discretization of 40 elements, 124 dofs are used for the nonlinear dynamic analysis of the curved beam. Besides, the total number of time steps is 100.

In the offline stage, the vectors of displacement and stiffness matrices corresponding to each time step are collected and assembled to the snapshots $\boldsymbol{U}_{snap}$ and $\boldsymbol{K}_{snap}$ which are then decomposed through SVD. The distributions of the singular values for the stiffness matrix and displacement field are shown in Fig 2(a) and (b), respectively. Rapid convergence rates are observed which signifies that only a few bases are needed for the proposed reduced order model.

In the online stage, the same time span and number of time steps are used as the offline stage. The number of base vectors (i_u=10, i_k=12) of displacement and stiffness matrices are determined by (13)

and the value of τ . The nonzero items of the stiffness matrix of full order model and the reduced order model are shown intuitively in Fig 2(c) and (d), respectively. It can be seen that only 12 entries are needed for the ROM, while the number of involved elements is 22 (as shown in Table 1), which is mainly due to the large support size of the NURBS basis.

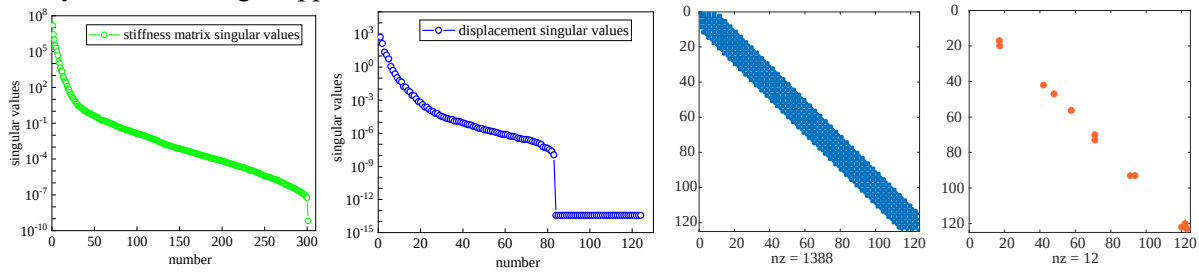

Figure 2. Distribution of singular values and nonzero items in stiffness matrix of spiral beam. (a) Stiffness matrix singular values. (b) Displacement singular values. (c) Nonzero items in the stiffness matrix of full order model. (d) Nonzero items in the stiffness matrix of reduced order model, nz is the number of nonzero items.

For comparison, Abaqus solutions of both linear and geometrically nonlinear elements (B21), together with the nonlinear dynamic responses of the FOM and ROM are shown in Fig 3(a). The displacement difference in the x and y directions in Fig 3(b) demonstrates that the calculation results of the full order model and reduced order model agree well, which indicates the accuracy of the proposed reduced order model.

Table 1. DEIM interpolation positions for the stiffness matrix of the spiral beam

Position ϕ_i	Row index of $\boldsymbol{K}_T$	Column index of $\boldsymbol{K}_T$	Involved elements	Position ϕ_i	Row index of $\boldsymbol{K}_T$	Column index of $\boldsymbol{K}_T$	Involved elements
2001	17	17	5,6,7,8	8572	72	71	23,24,25,26
2002	18	17	5,6,7,8	11377	93	92	30,31,32,33
5002	42	41	13,14,15,16	11501	93	93	30,31,32,33
5751	47	47	15,16,17,18	15126	122	122	40
7001	57	57	18,19,20,21	15127	123	122	40
8751	71	71	23,24,25,26	15251	123	123	40

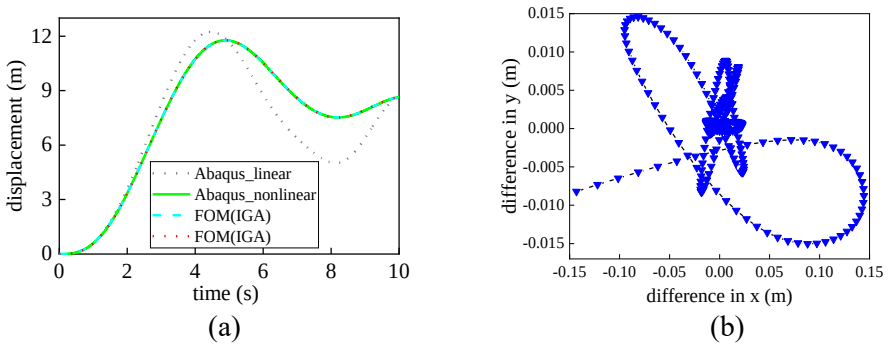

Figure 3. Displacement and displacement difference between full order model and reduced order model of the spiral beam. (a) Displacement. (b) Displacement difference.

4.2. Cylindrical shell

In this example, a simply supported cylindrical shell subjected to a centrally located concentrated force is studied. The geometric descriptions and material properties are given in Fig 1(b). The shell is discretized with 267dofs and 60 elements, with 10 and 6 elements in the circumferential and axial directions, respectively. The polynomial orders in two parametric directions are chosen as p=q=3.

In the offline stage, the time step size is set to be 0.01. Then, the snapshots $\boldsymbol{U}_{snap}$ and $\boldsymbol{K}_{snap}$ are collected. Fig 4 demonstrates the distribution of the singular values of SVD($\boldsymbol{U}_{snap}$) and SVD($\boldsymbol{K}_{snap}$).

In the online stage, the same time span and time step size are kept as the offline stage. The number of base vectors (i_u=22, i_k=9) of displacement and stiffness matrix are determined by (13) and the value of τ . The nonzero items of the stiffness matrix of full order model and the reduced order model are shown intuitively in Fig 4(c) and (d), respectively. It can be seen that only 9 positions are need for the ROM, while the number of involved elements is 46, which is mainly due to the tensor product of NURBS basis has larger support size than single NURBS basis.

For comparison, Fig 5(a) shows displacement responses obtained with the Abaqus (S4R) linear and geometrically nonlinear elements, as well as the IGA-based ROM and FOM. The comparisons of displacement and frequency responses in Fig 5 confirms the accuracy of the proposed model order reduction method.

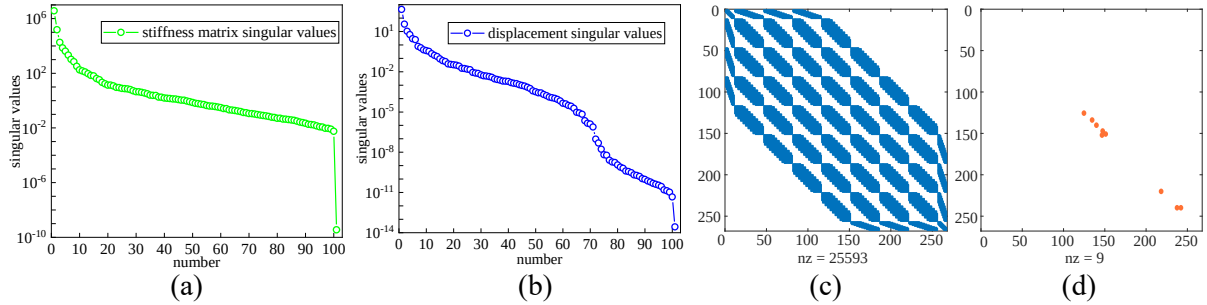

Figure 4. Distribution of singular values and nonzero items in stiffness matrix of cylindrical shell. (a) Stiffness matrix singular values. (b) Displacement singular values. (c) Nonzero items in the stiffness matrix of full order model. (d) Nonzero items in the stiffness matrix of reduced order model, nz is the number of nonzero items.

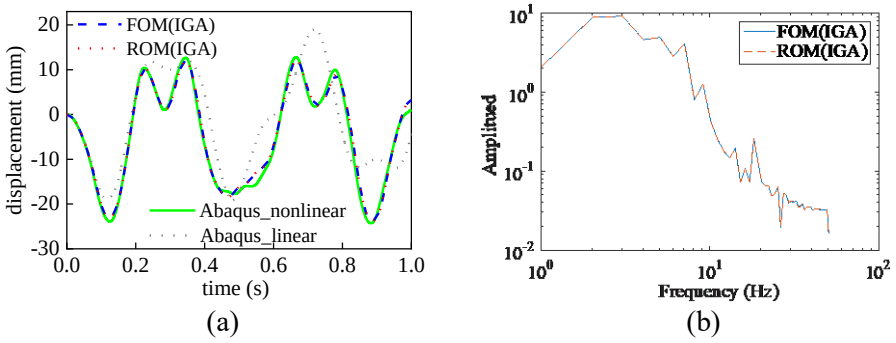

Figure 5. Displacement and frequency comparison between full order model and reduced order model of the cylindrical shell. (a) Displacement. (b) Frequency response.

5. Summary

In this paper, model order reduction of structural nonlinear dynamics is studied based on the isogeometric analysis. Proper orthogonal decomposition of the displacement field is used for the dimensional reduction. To deal with the nonlinearities of the stiffness matrix, discrete empirical interpolation method combined with POD is adopted to further reduce the computational burden of the ROM. Based on the proposed method, only a few entries of the stiffness matrix are needed for the reconstruction of the full stiffness matrix which significantly improves the computational efficiency of

the structural nonlinear dynamic analysis. Numerical examples of planar curved beam and 3D cylindrical shell problems confirm the accuracy and efficiency of the proposed method.

Acknowledgements
The authors would like to thank the National Natural Science Foundation of China (Grant no. 11972187, 12002161) for their support.

References
[1] Chaturanabut S. Nonlinear model reduction via discrete empirical interpolation [D]. USA: Rice University, 2011.
[2] Barrault M, Maday Y, Nguyen N C, et al. An 'empirical interpolation' method: application to efficient reduced basis discretization of partial differential equations [J]. Comptes Rendus Mathematique, 2004, 339: 667—672.
[3] Grepl M A, Maday Y, Nguyen N C, et al. Efficient reduced-basis treatment of nonaffine and nonlinear partial differential equations [J]. Mathematical Modelling and Numerical Analysis, 2007, 41: 575—605.
[4] Yao W, Marques S. Nonlinear Aerodynamic and Aeroelastic Model Reduction using a Discrete Empirical Interpolation Method[J]. AIAA Journal, 2017, 55(2):1-14.
[5] Ghavamian F, Tiso P, Simone A. POD-DEIM model order reduction for strain softening viscoplasticity[J]. Computer Methods in Applied Mechanics & Engineering, 2017, 317(APR.15):458-479.
[6] Guo Y, Wu H, Li W. Model order reduction for nonlinear dynamic analysis of parameterized curved beam structures based on Isogeometric analysis[J]. Engineering mechanics. doi: 10.6052/j.issn.1000-4750.2021.04.0285
[7] Hughes T, Cottrell J A, Bazilevs Y. Isogeometric analysis: CAD, finite elements, NURBS, exact geometry and mesh refinement[J]. Computer Methods in Applied Mechanics & Engineering, 2005, 194(39-41):4135-4195.
[8] Weeger O , Wever U , Simeon B . Isogeometric analysis of nonlinear Euler-Bernoulli beam vibrations[J]. Nonlinear Dynamics, 2013, 72(4):813-835.
[9] Kiendl J, Bletzinger K U, Linhard J, et al. Isogeometric shell analysis with Kirchhoff–Love elements[J]. Computer Methods in Applied Mechanics & Engineering, 2009, 198(49-52):3902-3914.
[10] Wriggers P . Nonlinear Finite Element Analysis of Solids and Structures[J]. Journal of Engineering Mechanics, 1991, 17(6):1504-1505.